Robust 3D rotation invariant local binary pattern for volumetric texture classification

Shengyu Lu*, Sasan Mahmoodi and Mahesan Niranjan
School of Electronics and Computer Science
University of Southampton
Southampton, United Kingdom
Email: Shengyu Lu@soton.ac.uk, sm3@ecs.soton.ac.uk, mn@ecs.soton.ac.uk

***Abstract*—3D local binary pattern (LBP) shows significant performance in many domains such as solid textures analysis, face recognition and tumor detection. In recent years, rotation invariant 3D LBP texture descriptors have received increasing attention and several variants have been proposed. However, they are sensitive to the noise present in the image. In this paper, we propose an efficient rotation invariant texture descriptor known as robust extended 3D LBP (*RELBP*) for volumetric texture classification. Unlike the current 3D LBP framework, our descriptor uses the information of neighboring voxels to reduce noise. First, the 3D weighted average filter is employed to process each voxel in the image, in which the center voxel is replaced by the average local gray level based on weights. Besides, equidistant points on a sphere are sampled to construct a set of rotation invariant features. Our experiments demonstrate that the *RELBP* proposed here shows superior classification performance in texture classification tasks and our method is highly robust to image noise on benchmark datasets.**

Keywords—3D local binary pattern (3D LBP); volumetric texture; texture descriptors

I. INTRODUCTION

Texture analysis plays a significant role in image processing and pattern recognition, especially in medical applications [1]. Texture descriptors provide rich information about the characterization and properties of objects or regions in various types of images [2]. In the past decades, many texture feature extraction methods have been proposed [3] and successfully employed in many domains such as human detection, medical image analysis and face recognition [4]. Encoding high discriminant descriptors is essential to address specific tasks, but feature extraction may be affected by noise and some image transformations such as rotation and translation [5]. In order to overcome such issues, researchers have proposed some strategies to make the texture model more robust [6]. However, most of these techniques are developed to capture robust texture descriptors in 2D images and there are a few approaches proposed for 3D texture analysis [7]. Compared to 2D images [8], 3D volumetric images contain rich spatial information and usually lead to algorithms with more superior performances in many applications such as brain tumor detection in magnetic resonance imaging (MRI) [9]. Therefore, extending 2D texture analysis methods to characterize 3D images is pretty valuable, but such an extension faces many challenges such as increases in computation time and the presence of noise interference [10].

Local binary pattern (LBP) descriptor was initially proposed by Ojala et al. for 2D texture analysis and demonstrates superior performance in texture classification and segmentation tasks [11]. Due to its outstanding advantages of easy implementation and low computational complexity, LBP has been widely used for texture analysis in the past decade and various variants for LBP have been put forward to improve its model capabilities [12][13][16][14][15]. For example, Guo et al. developed a completed LBP (*CLBP*) scheme that combined the sign and magnitude components to encode the texture descriptors and improve its discriminative power [3]. Rakesh Mehta and Karen Egiazarian proposed a novel texture descriptor known as *DRLBP* that captured both the structural information and magnitude information in a local pattern to extract rotation invariant features and improve classification performance [2]. Although much progress has been made, these algorithms are usually applied in 2D texture analysis and few 3D LBP variants are proposed to match the requirements.

The main challenges for 3D LBP descriptors are to deal with rotation invariance [16] and noise sensitivity [17]. Some approaches have been proposed to construct 3D rotation invariant LBP descriptors to overcome image orientation [16]. For example, Citraro et al. proposed an Icosahedron spherical structure to sample equidistant points and used "Uniform" patterns to achieve rotation invariance [1]. J. Fehr and H. Burkhardt proposed a novel method that constructed a sphere and employed spherical harmonics to calculate rotation invariant 3D LBP descriptors [18]. Although scholars have presented some strategies to improve the noise-tolerance property of LBP methods, those approaches are only limited to 2D texture analysis. For example, Fathi et al. presented a noise-tolerant LBP descriptor that used a circular majority voting filter and labeling scheme to improve model robustness and discrimination ability [19]. Based on the uniform LBP, Chen et al. proposed a robust texture descriptor by changing the coding of the three-bit substring to make the model more robust against noise [20]. Nonetheless, as far as we know, there is no robust 3D LBP descriptor in the literature.

The main contribution of this paper is to propose an efficient 3D LBP descriptor to achieve rotation invariance and improve noise tolerance. To the best of our knowledge, this is the first

work in which a robust texture descriptor is proposed to overcome the noise sensitivity issue in the 3D LBP framework. For each voxel in the 3D images, we employ a 3D weighted average filter that replaces its original gray scale value with the average local voxel based on weights to reduce the influence of noise. In addition, inspired by the extended LBP (*ELBP*) variant, we combine the texture features of center intensity-based (*CI*), neighborhood intensity-based (*NI*) and radial difference-based (*RD*) descriptors to enhance model robustness and classification performance [21]. In order to construct rotation invariant descriptors, we distribute equidistant neighboring points on the sphere surrounding the center voxel to encode uniform and non-uniform patterns. Unlike deep convolutional neural networks, our method only requires a small number of training samples and enjoys low computational costs. More importantly, our method proposed here demonstrates strong robustness, to image orientation and noise contamination. Therefore, the robust extended 3D LBP method (*RELBP*) is suitable for small datasets such as medical images. Our experimental results illustrate that the *RELBP* method achieves excellent classification performance in volumetric texture classification and is robust to image noise in public datasets.

II. Related Work

A. 3D local binary pattern

Zhao and Pietikäinen first introduced the concept of 3D LBP by proposing volume LBP (*VLBP*) descriptors to extract the texture features in a local neighborhood of the center volume [22]. Then Paulhac et al. proposed a rotation invariant 3D LBP descriptor known as LBP^{riu3} that constructed a sphere for each voxel to encode texture values with "Uniform" patterns [16], which is the most popular 3D LBP variant in the literature. In details, given a voxel v_c in the image, the LBP value is calculated by binary encoding the differences between v_c and its neighboring point v_i. In 3D space, neighboring points are uniformly sampled from a series of circles in a sphere. Each vertex v_c in the sphere is assigned a gray value based on the bilinear interpolation of several neighboring voxels. We let s represent the number of circles and p is the number of vertexes in each circle. $p' = (s-2) \times p + 2$ denotes the number of neighbors for the center voxel. Formally, the 3D LBP descriptor is defined as follows:

$$LBP = \begin{cases} \sum_{i=0}^{p-1} f(v_i - v_c) & if\ U \le V \\ p & else\ U > V \end{cases} \quad (1)$$

where

$$f(x) = \begin{cases} 1 & if\ \ x \ge 0 \\ 0 & else\ \ x < 0 \end{cases} \quad (2)$$

and

$$U = |f(v_{p-1} - v_c) - f(v_0 - v_c)| + \sum_{i=1}^{p-1} |f(v_i - v_c) - f(v_{i-1} - v_c)| \quad (3)$$

In equations (1) to (3), U represents the measurement that counts the number of bit transitions from 1 to 0 or vice versa. V denotes the threshold that defines the LBP as "uniform" or "non-uniform".

B. 3D extended local binary pattern

Since the original LBP only captures the relationship between the center point and its neighbors, some spatial relationships in a local region may be lost. To resolve this issue, Liu et al. proposed a novel method known as *ELBP* which consisted of three different LBP descriptors referred to *CI*, *NI*, *RD* to extract more distinctive spatial information and to improve classification performance for 2D texture analysis [21]. Then Citraro et al. extended this framework to 3D space ($NI/RD/CI\text{-}LBP^{riu3}$) by constructing a sphere for each voxel and uniformly searching for neighboring points on the sphere to calculate *CI*, *NI*, *RD* descriptor [1]. The first descriptor *CI* encodes the contrast information between the center voxel v_c and the mean of the whole image m:

$$CI_{p,r} = f(v_c - m) \quad (4)$$

Another LBP descriptor *NI* uses the mean value n of neighboring points as the threshold instead of the center voxel to calculate the LBP value, i.e.:

$$NI_{p,r} = \begin{cases} \sum_{i=0}^{p-1} f(v_i - n) & if\ U \le V \\ p & else\ U > V \end{cases} \quad (5)$$

with $n = \frac{1}{p}\sum_{i=0}^{p-1} v_i$.

The final descriptor *RD* encodes the voxel differences in radial directions:

$$RD_{p,r} = \begin{cases} \sum_{i=0}^{p-1} f(v_i^r - v_i^{r-1}) & if\ U \le V \\ p & else\ U > V \end{cases} \quad (6)$$

III. Method

A. Uniform spherical sampling

A rotation invariant 3D LBP descriptor is not expected to change under all points of camera view. Searching for minimum LBP over all angles of the neighboring points with fixed weights in 3D space leads to high computational complexity [18]. In addition, this strategy does not provide very good discrimination. Motived by "Uniform" patterns [11], we assign the same weight to the neighbors from different angles to achieve rotation invariance. A significant step toward constructing rotation invariant descriptors is to sample equidistant points on the sphere. However, it is not trivial to construct such a geometrical structure in a spherical neighborhood [23]. Citraro et al. developed a geodesic sphere that subdivided the surface in uniform flat polygonal faces to achieve equidistant neighboring points sampling [1]. However, the number of points is limited to specific values. In this paper, we adopt a solution where equidistant and unlimited number of vertices (p) are placed on the sphere surrounding the center

voxel. In details, we choose circles of latitude at constant intervals d_θ and sample points on those circles at constant intervals d_φ, such that $d_\theta \approx d_\varphi$ and $p \times (d_\theta \times d_\varphi)$ equals to the area of the sphere [24]. The configuration of voxels in a spherical neighborhood is shown in Fig. 1. Then we use the gray values of the center voxel v_c and neighboring points v_i to encode texture patterns.

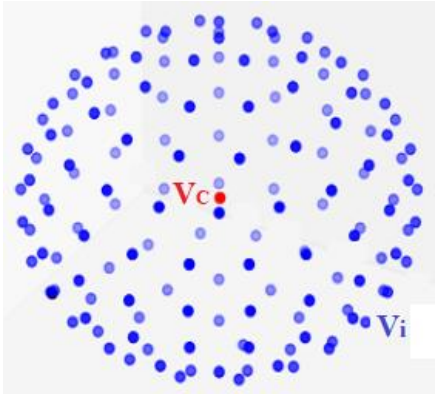

Fig. 1. A center voxel and spherical neighbourhood in 3D space.

B. Robust 3D extended local binary pattern descriptors

Although 3D LBP has high discriminative power, it is very vulnerable to image noise and such a noise sensitivity for the 3D LBP framework has not been addressed in the literature. In order to reduce the influence of noise present in images, we consider a weighted average function $g(v_c|\, w,p)$ for each voxel v_c in the image to make the model more robust against noise [3] as presented in equation (7):

$$g(v_c|\, w,p) = \frac{\sum_{i=0}^{p-1}(v_i + v_c \times w)}{w+p} \tag{7}$$

where, p is the number of neighboring points around the center voxel and w represents the weight of the center voxel. Such voxel contains more valuable information than its neighbors. By calculating the mean gray value based on weights, instead of the original gray scale value of the central voxel, we can reduce the influence of noise.

We use individual central voxel with regional representation in LBP value calculations and consider three robust texture descriptors.

Robust *CI* (*RCI*) descriptor is defined as follows:

$$RCI_{p,r,w} = f(g(v_c|w,p) - \propto) \tag{8}$$

where, $\propto$ is the mean voxel of the whole image processed by the weighted average function $g(v_c|w,p)$.

Robust *NI* (*RNI*) descriptor is defined as:

$$RNI_{p,r,w} = \begin{cases} \sum_{i=0}^{p-1} f(g(v_i|w,p) - \propto_c) & if\ U \le V \\ p & else\ U > V \end{cases} \tag{9}$$

where

$$\propto_c = \frac{1}{p}\sum_{i=0}^{p-1} g(v_i|w,p) \tag{10}$$

Robust *RD* (*RRD*) descriptor is presented as:

$$RRD_{p,r,w} = \begin{cases} \sum_{i=0}^{p-1} f(g(v_i^{r+1}|w,p) - g(v_i^{r}|w,p)) & if\ U \le V \\ p & else\ U > V \end{cases} \tag{11}$$

After the LBP value of each voxel $v_{i,j,k}$ in the image is calculated, we compute a histogram $H(b)$, $b \in [0,B]$ to represent the texture descriptor.

$$H(b) = \sum_{i=1}^{I}\sum_{j=1}^{J}\sum_{k=1}^{K} \varphi(LBP_{i,j,k}, b) \tag{12}$$

and

$$\varphi(\alpha,\beta) = \begin{cases} 1 & if\ \alpha = \beta \\ 0 & else \end{cases} \tag{13}$$

where, B denotes the maximum LBP value in a texture image.

We calculate the histograms of the *RCI*, *RNI* and *RRD* descriptors respectively, and then concatenate these three histograms together to construct a feature vector of a texture. Among machine learning classifiers, k-nearest neighbors is adopted to achieve volumetric texture classification with the following texture feature:

$$H = H_{RCI} \oplus H_{RNI} \oplus H_{RRD} \tag{14}$$

where $\oplus$ represents concatenation operation.

C. Multi-scale analysis

Ojala et al. stated that multi-resolution analysis by combining the operators of various (p, r) could improve the classification performance of the LBP method for 2D texture analysis [11]. In this paper, we apply this strategy to the *RELBP* method to improve its discriminative capability. In details, we vary the radius r of the sphere surrounding the center voxel but sample the same number of neighboring points p. Then we calculate multiple *RCI*, *RNI* and *RRD* operators in various r and concatenate their histograms together.

IV. Experiments

In order to evaluate the discriminative power and model robustness of our proposed *RELBP* method for 3D texture analysis, we perform a series of experiments on two different datasets, comparing to state-of-the-art methods.

A. Datasets

There is no standard 3D texture dataset for the evaluation of classification performance. As a result, researchers usually use datasets containing synthetic or real images to compare the performance of various 3D texture analysis methods. In this

paper, we use two public datasets to make an effective comparison.

The first one is the RFAI database[1] that is synthetically constructed from 2D images by using four different methods [25]. The first method produces a 3D texture image by interpolating several 2D texture images. The second method employs geometric shapes such as cubes to generate 3D textures. In the third method, Fourier transformation is used to construct volumetric 3D textures. The final one mixes the three previous methods to synthesize a 3D image. Four categories named as "Interpolated", "Geometric", "Fourier" and "Mixed texture" are produced by these four image synthesis methods. Each category comprises five kinds of textures according to image distortion, including normal, noise, rotation, blurry and subsampling. We use the normal, noise and rotation subsets of the "Mixed texture" category which contains 25 classes to evaluate the performance of our method. There are 10 examples in each kind of texture and their size is $64 \times 64 \times 64$.

The realistic COVID dataset[2] is CT images of the lung. It is used to evaluate 3D texture analysis methods in classifying COVID-19 and non-COVID-19 on CT scans. We pick 10 CT images of COVID-19 and non-COVID-19 respectively, from the COVID database. For each CT scan, we select two $32 \times 32 \times 32$ image patches from left and right lung regions respectively. Therefore, the COVID dataset contains 80 samples.

B. Metrics and settings

To evaluate the noise-tolerance property of all methods, we add zero mean Gaussian noise with different intensities to volumetric images respectively. The signal-to-noise ratio (SNR) is used to represent the amount of noise contaminating 3D textures. Our experiments have been performed at SNR=20, 10 6 and 5 respectively on RFAI and COVID datasets to compare the robustness of methods investigated here. We take 80% texture images for training and the remaining 20% for testing. The data is divided into five equal parts randomly using five-folder cross validation. Our proposed *RELBP* method is examined by classification accuracy and F1 score. The F1 score is the harmonic mean of precision and recall, which is defined as follows:

$$\text{precision} = \frac{TP}{TP + FP} \tag{15}$$

$$\text{recall} = \frac{TP}{TP + FN} \tag{16}$$

$$\text{F1} = \frac{2 \times \text{precision} \times \text{recall}}{\text{precision} + \text{recall}} \tag{17}$$

Where, *TP*, *FP*, *FN* represent the true positive, false positive and false negative respectively.

The $3 \times 3 \times 3$ weighted average filter is used to process each voxel in the image ($p = 26$) and the weight of the center voxel w is set to 26. In terms of the k-nearest neighbors algorithm, we use the Manhattan distance to emphasize the discriminatory power of each descriptor, and $k = 1$ is selected for the texture classification task. Using the uniform spherical sampling scheme, we develop several 3D LBP variants and compare them with the *RELBP* method. The parameter settings for our various methods in this paper are as follows:

a) RELBP: The radius r of the sphere constructed for each voxel is set to 1 and we sample 12 uniformly distributed points on the sphere (p=12). The number of histogram bins of *RCI*, *RNI* and *RRD* descriptors are selected as 2, 14 and 14, respectively.

b) Multi-scale RELBP (MS-RELBP): Here we combine multiple *RELBP* descriptors from various scales for 3D texture analysis. We use two groups represented by various values for (p, r), i.e. i) p=12, r=1 and ii) p=12, r=2 to calculate texture descriptors respectively and these three descriptors are then concatenated to be used in classification.

c) Robust rotation invariant LBP (RRI-LBP): It is the traditional 3D LBP descriptor with "Uniform" patterns to encode the differences between the center voxel v_c and its neighbors v_i . Similarly to the *RELBP* descriptor (p=12, r=1), we use the weighted average function to process the volumetric image to reduce noise. The threshold is the weighted average of the gray value of the center voxel and its neighboring points, and the weight of v_c is set to 12.

C. Results and discussion

To make an efficient evaluation, we compare the classification performance with other state-of-the-art 3D LBP variants. The first one is the $VLBP^{riu2}$ descriptor proposed by Zhao and Pietikäinen to process each sequence of dynamic textures via minimum search over circular bitwise right shifts for rotation invariant classification [22]. The second method *LBP-TOP*, only uses the co-occurrences of the LBP descriptors on three orthogonal planes and concatenates their histograms for volumetric texture classification [26]. This descriptor has low computational costs and superior discriminative capability, but lacks the rotation invariant property. The remaining two 3D rotation invariant LBP descriptors LBP^{riu3} and *NI/RD/CI-*LBP^{riu3} are as introduced in related work. To evaluate the model capability between *RELBP* and other 3D LBP variants fairly, the parameters of comparison methods are assigned as follows:

a) $VLBP^{riu2}$*:* Three consecutive frames are stacked to encode the binary codes. We select 14 neighboring voxels for each center voxel [22].

b) LBP-TOP: For each plane, we uniformly sample 8 neighboring vertices in a circle and set the radius to 1. The value of concatenated histogram bins from three orthogonal planes is 48 [26].

c) LBP^{riu3}*:* Unity for radius, 8 for the number of points in each circle, 5 for the number of circles and 26 for the number of uniform patterns [16].

d) NI/RD/CI-LBP^{riu3}*:* We employ the same parameter settings as the *RELBP* descriptor [1].

[1]http://www.rfai.li.univ-tours.fr/fr/ressources/3Dsynthetic_images_database.html
[2]https://aistudio.baidu.com/aistudio/datasetdetail/34221

TABLE I. CLASSIFICATION PERFORMANCE OF VARIOUS METHODS WITH GAUSSIAN NOISE ON THE RFAI DATASET

Method	Accuracy				F1			
	SNR=20	SNR=10	SNR=6	SNR=5	SNR=20	SNR=10	SNR=6	SNR=5
RELBP	0.99 ± 0.01	0.96 ± 0.02	$\mathbf{0.88 \pm 0.03}$	$\mathbf{0.82 \pm 0.03}$	0.99 ± 0.01	0.96 ± 0.02	$\mathbf{0.86 \pm 0.04}$	$\mathbf{0.79 \pm 0.02}$
RRI-LBP	0.99 ± 0.01	0.92 ± 0.02	0.70 ± 0.06	0.60 ± 0.04	0.99 ± 0.01	0.91 ± 0.02	0.68 ± 0.06	0.57 ± 0.05
$VLBP^{riu2}$	0.98 ± 0.01	0.80 ± 0.04	0.50 ± 0.06	0.38 ± 0.04	0.97 ± 0.01	0.78 ± 0.04	0.48 ± 0.06	0.37 ± 0.03
LBP-TOP	$\mathbf{1.00 \pm 0.00}$	$\mathbf{0.97 \pm 0.03}$	0.63 ± 0.03	0.52 ± 0.05	$\mathbf{1.00 \pm 0.00}$	0.96 ± 0.02	0.59 ± 0.04	0.50 ± 0.03
LBP^{riu3}	0.98 ± 0.01	0.92 ± 0.02	0.74 ± 0.06	0.72 ± 0.06	0.98 ± 0.01	0.91 ± 0.03	0.75 ± 0.06	0.69 ± 0.06
$NI/RD/CI\text{-}LBP^{riu3}$	0.99 ± 0.01	$\mathbf{0.97 \pm 0.02}$	0.81 ± 0.05	0.64 ± 0.03	0.99 ± 0.01	$\mathbf{0.97 \pm 0.02}$	0.79 ± 0.06	0.61 ± 0.03

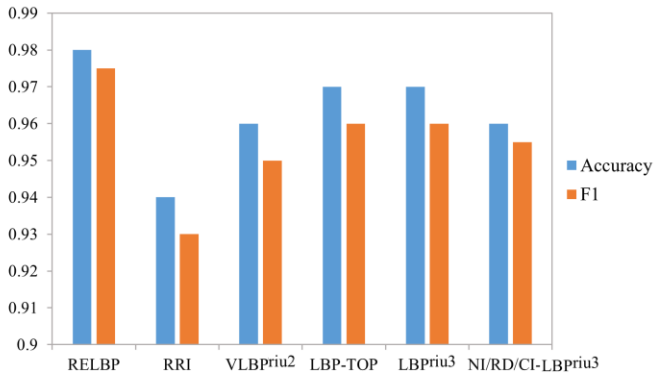

Fig. 2. Comparing the classification performance of all methods on the noise subset of the RFAI dataset.

To examine the noise-tolerant property of all methods, we compare their classification performance on the noise subset of the RFAI dataset. This subset is synthesized using 2D images with unknown kinds of noise. Classification accuracies and F1 scores displayed in Fig. 2 indicate that the *RELBP* has stronger model robustness against noise than other 3D LBP variants. Furthermore, we add zero mean Gaussian noise to the normal subset of the RFAI dataset to form noisy volumetric textures with various SNRs and evaluate the performances. Table I compares the accuracies and F1 scores of different 3D LBP variants at the presence of additive zero mean Gaussian noise. We can see that our proposed *RELBP* descriptor is more robust against noise than other state-of-the-art LBP variants. All methods have excellent classification performance in the images with small noise. However, when SNR is less than 6, our method has obvious advantages and retains high accuracy. Compared with the *RRI-LBP* variant, our *RELBP* descriptor that combines the information of *RCI*, *RNI* and *RRD* operators has better discriminative capability and model robustness.

We evaluate our *RELBP* method proposed here further by setting various weights w for the center voxel in the 3D weighted average filter. Table II demonstrates the experimental results on the normal subset contaminated with zero mean additive Gaussian noise (SNR=10). We can find that our method achieves the best performance when w is set to 13. Although the center voxel contains more valuable information than its neighbors, the weight should not be assigned too large.

TABLE II. CLASSIFICATION PERFORMANCE FOR VARIOUS WEIGHTS w OF THE CENTER VOXEL USING THE NORMAL SUBSET WITH SNR=10

w	Accuracy
1	0.92 ± 0.04
13	$\mathbf{0.97 \pm 0.02}$
26	0.96 ± 0.03
39	0.96 ± 0.03

The rotation invariant property of our method is also investigated here on the rotation subset of the RFAI dataset. Each texture class of the rotation subset contains ten randomly rotated volumetric images. Fig. 3 illustrates the classification results of various 3D LBP variants on rotated images. Our proposed rotation invariant *RELBP* descriptor demonstrates excellent discriminative power, although texture images are rotated at random angles. In addition, the multi-scale strategy contributes to enhancing the classification performance of our *RELBP* descriptor.

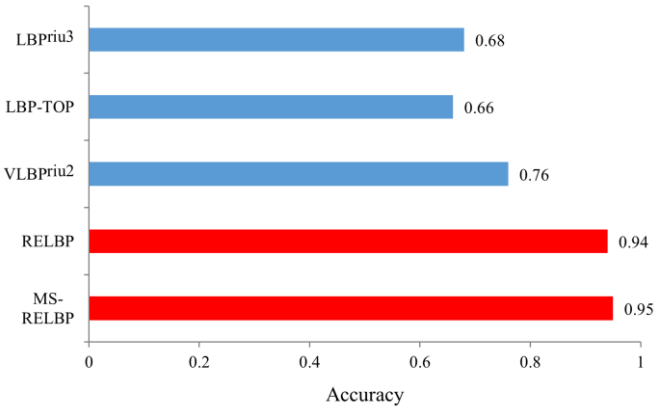

Fig. 3. Comparison of the classification accuracy obtained from various methods on the rotation subset of the RFAI dataset.

Fig. 4 depicts the classification performance of all 3D LBP variants using the COVID dataset. Our *RELBP* descriptor

enjoys strong model robustness to noise and its classification accuracy drops modestly when lung CT images are contaminated with additive zero mean Gaussian noise. However, $VLBP^{riu2}$ and *LBP-TOP* variants are very vulnerable to noise present in the images and perform poorly in COVID-19 detection. Compared with the *NI/RD/CI-*LBP^{riu3} variant, the 3D weighted average filter plays an essential role in improving the noise-tolerant property of our *RELBP* descriptor because the weighted average function reduces the impacts of noise on the center voxel when encoding texture patterns. In Fig. 5, we show the confusion matrix for our method on the same data with additive zero mean Gaussian noise (SNR=6). As observed in this figure, the proposed descriptor *RELBP* is robust to noise contamination and provides high accuracies in both categories.

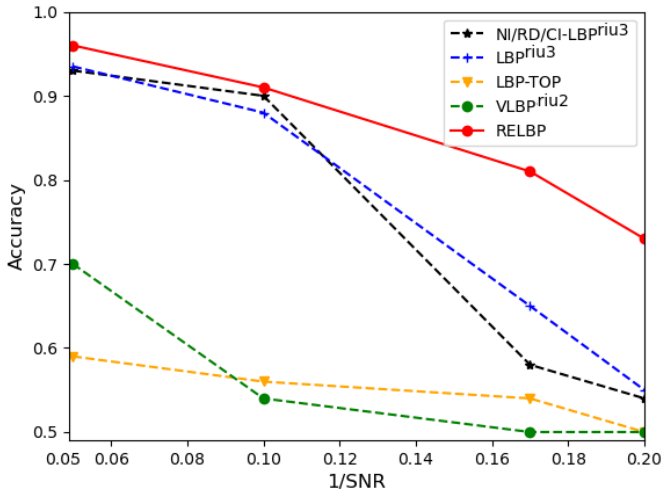

Fig. 4. Comparing the classification performance of all methods with Gaussian noise on the COVID dataset.

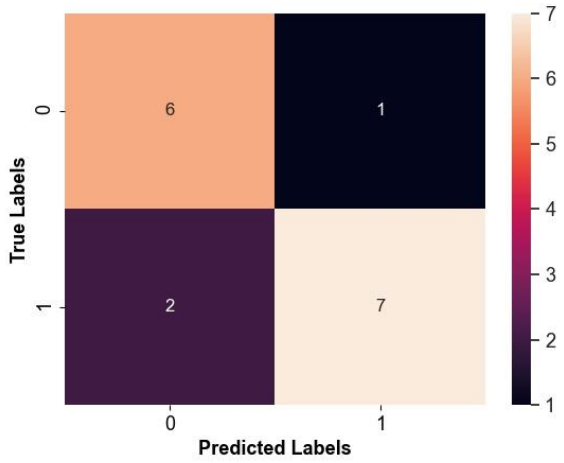

Fig. 5. Confusion matrix for our method using the COVID dataset with SNR=6.

Apart from the k-nearest neighbors classifier, other classification algorithms, including random forest, support vector machine and decision tree, are also used to evaluate the performance of our proposed descriptor. Table III presents the classification results of the *RELBP* method using various machine learning classifiers on the COVID dataset with additive zero mean Gaussian noise (SNR=10). We can see that all classifiers provide high accuracies in noisy images and random forest demonstrates the best performance with an accuracy of 0.95.

TABLE III. COMPARE THE CLASSIFICATION ACCURACY OF VARIOUS MACHINE LEARNING CLASSIFIERS ON THE COVID DATASET

Classifiers	**Accuracy**
k-nearest neighbors	0.91 ± 0.03
random forest	$\mathbf{0.95 \pm 0.03}$
support vector machine	0.93 ± 0.05
decision tree	0.94 ± 0.03

Our *RELBP* descriptor proposed here has excellent classification performance and model robustness in rotated and noisy images. In many practical applications such as medical imaging, not all images are scanned at a perfect angle and nor they may be free from noise. Our *RELBP* method can therefore be used in these tasks and it is robust against image perturbation caused by equipment or other uncertainties.

CONCLUSION

In this paper, we present a novel *RELBP* method for accurate and robust volumetric texture classification. Our method proposed here enhances the model robustness of 3D LBP at the presence of noise. The robust *RELBP* descriptor has strong noise tolerance, and also is invariant to rotation and illumination variations. Our experiments demonstrate that the *RELBP* method has superior discriminative power, and it outperforms recent state-of-the-art 3D LBP variants in noisy and rotated images. As future work, we are desired to extend our method presented here to 3D volumetric texture segmentation and object localization. We also expect the proposed method to be generalized to other domains and motivate new researchers to improve the noise-tolerant property of models.

ACKNOWLEDGMENTS

Shengyu Lu is supported by a scholarship granted by the China Scholarship Council. This work was funded by the Engineering and Physical Sciences Research Council, UK: project EP/S000356/1 "Artificial and Augmented Intelligence for Automated Scientific Discovery".

REFERENCES

[1] L. Citraro, S. Mahmoodi, A. Darekar, and B. Vollmer, 'Extended three-dimensional rotation invariant local binary patterns', *Image Vis. Comput.*, vol. 62, pp. 8–18, Jun. 2017, doi: 10.1016/j.imavis.2017.03.004.

[2] R. Mehta and K. Egiazarian, 'Dominant Rotated Local Binary Patterns (DRLBP) for texture classification', Pattern Recognit. Lett., vol. 71, pp. 16–22, Feb. 2016, doi: 10.1016/j.patrec.2015.11.019.

[3] Y. Zhao, W. Jia, R.-X. Hu, and H. Min, 'Completed robust local binary pattern for texture classification', Neurocomputing, vol. 106, pp. 68–76, Apr. 2013, doi: 10.1016/j.neucom.2012.10.017.

[4] L. Nanni, A. Lumini, and S. Brahnam, ‘Survey on LBP based texture descriptors for image classification’, Expert Syst. Appl., vol. 39, no. 3, pp. 3634–3641, Feb. 2012, doi: 10.1016/j.eswa.2011.09.054.

[5] R. Maani, S. Kalra, and Y.-H. Yang, ‘Noise robust rotation invariant features for texture classification’, Pattern Recognit., vol. 46, no. 8, pp. 2103–2116, Aug. 2013, doi: 10.1016/j.patcog.2013.01.014.

[6] Z. Zhu et al., ‘An adaptive hybrid pattern for noise-robust texture analysis’, Pattern Recognit., vol. 48, no. 8, pp. 2592–2608, Aug. 2015, doi: 10.1016/j.patcog.2015.01.001.

[7] J. Xu, M. Cha, J. L. Heyman, S. Venugopalan, R. Abiantun, and M. Savvides, ‘Robust local binary pattern feature sets for periocular biometric identification’, in 2010 Fourth IEEE International Conference on Biometrics: Theory, Applications and Systems (BTAS), Washington, DC, USA, Sep. 2010, pp. 1–8. doi: 10.1109/BTAS.2010.5634504.

[8] Y. Almakady, S. Mahmoodi, J. Conway, and M. Bennett, ‘Rotation invariant features based on three dimensional Gaussian Markov random fields for volumetric texture classification’, Comput. Vis. Image Underst., vol. 194, p. 102931, May 2020, doi: 10.1016/j.cviu.2020.102931.

[9] D. Wang, Y. Zhang, K. Zhang, and L. Wang, ‘FocalMix: Semi-Supervised Learning for 3D Medical Image Detection’, in 2020 IEEE/CVF Conference on Computer Vision and Pattern Recognition (CVPR), Seattle, WA, USA, Jun. 2020, pp. 3950–3959. doi: 10.1109/CVPR42600.2020.00401.

[10] X. Liu, F. Hou, H. Qin, and A. Hao, ‘Multi-view multi-scale CNNs for lung nodule type classification from CT images’, Pattern Recognit., vol. 77, pp. 262–275, May 2018, doi: 10.1016/j.patcog.2017.12.022.

[11] T. Ojala, M. Pietikainen, and T. Maenpaa, ‘Multiresolution gray-scale and rotation invariant texture classification with local binary patterns’, IEEE Trans. Pattern Anal. Mach. Intell., vol. 24, no. 7, pp. 971–987, Jul. 2002, doi: 10.1109/TPAMI.2002.1017623.

[12] L. Liu, S. Lao, P. W. Fieguth, Y. Guo, X. Wang, and M. Pietikainen, ‘Median Robust Extended Local Binary Pattern for Texture Classification’, IEEE Trans. Image Process., vol. 25, no. 3, pp. 1368–1381, Mar. 2016, doi: 10.1109/TIP.2016.2522378.

[13] X. Qi, R. Xiao, C.-G. Li, Y. Qiao, J. Guo, and X. Tang, ‘Pairwise Rotation Invariant Co-Occurrence Local Binary Pattern’, IEEE Trans. Pattern Anal. Mach. Intell., vol. 36, no. 11, pp. 2199–2213, Nov. 2014, doi: 10.1109/TPAMI.2014.2316826.

[14] H. Zhou, R. Wang, and C. Wang, ‘A novel extended local-binary-pattern operator for texture analysis’, Inf. Sci., vol. 178, no. 22, pp. 4314–4325, Nov. 2008, doi: 10.1016/j.ins.2008.07.015.

[15] Z. Pan, Z. Li, H. Fan, and X. Wu, ‘Feature based local binary pattern for rotation invariant texture classification’, Expert Syst. Appl., vol. 88, pp. 238–248, Dec. 2017, doi: 10.1016/j.eswa.2017.07.007.

[16] L. Paulhac, P. Makris, and J.-Y. Ramel, ‘Comparison between 2D and 3D Local Binary Pattern Methods for Characterisation of Three-Dimensional Textures’, in Image Analysis and Recognition, vol. 5112, A. Campilho and M. Kamel, Eds. Berlin, Heidelberg: Springer Berlin Heidelberg, 2008, pp. 670–679. doi: 10.1007/978-3-540-69812-8_66.

[17] Xiaoyang Tan and B. Triggs, ‘Enhanced Local Texture Feature Sets for Face Recognition Under Difficult Lighting Conditions’, IEEE Trans. Image Process., vol. 19, no. 6, pp. 1635–1650, Jun. 2010, doi: 10.1109/TIP.2010.2042645.

[18] J. Fehr and H. Burkhardt, ‘3D rotation invariant local binary patterns’, in 2008 19th International Conference on Pattern Recognition, Tampa, FL, USA, Dec. 2008, pp. 1–4. doi: 10.1109/ICPR.2008.4761098.

[19] A. Fathi and A. R. Naghsh-Nilchi, ‘Noise tolerant local binary pattern operator for efficient texture analysis’, Pattern Recognit. Lett., vol. 33, no. 9, pp. 1093–1100, Jul. 2012, doi: 10.1016/j.patrec.2012.01.017.

[20] J. Chen, V. Kellokumpu, G. Zhao, and M. Pietikainen, ‘RLBP: Robust Local Binary Pattern’, in Procedings of the British Machine Vision Conference 2013, Bristol, 2013, p. 122.1-122.11. doi: 10.5244/C.27.122.

[21] L. Liu, L. Zhao, Y. Long, G. Kuang, and P. Fieguth, ‘Extended local binary patterns for texture classification’, Image Vis. Comput., vol. 30, no. 2, pp. 86–99, Feb. 2012, doi: 10.1016/j.imavis.2012.01.001.

[22] G. Zhao and M. Pietikäinen, ‘Dynamic Texture Recognition Using Volume Local Binary Patterns’, in Dynamical Vision, vol. 4358, R. Vidal, A. Heyden, and Y. Ma, Eds. Berlin, Heidelberg: Springer Berlin Heidelberg, 2007, pp. 165–177. doi: 10.1007/978-3-540-70932-9_13.

[23] J. Banerjee, A. Moelker, W. J. Niessen, and T. van Walsum, ‘3D LBP-Based Rotationally Invariant Region Description’, in Computer Vision - ACCV 2012 Workshops, vol. 7728, J.-I. Park and J. Kim, Eds. Berlin, Heidelberg: Springer Berlin Heidelberg, 2013, pp. 26–37. doi: 10.1007/978-3-642-37410-4_3.

[24] M. Deserno, ‘How to generate equidistributed points on the surface of a sphere’, p. 1.

[25] ‘A SOLID TEXTURE DATABASE FOR SEGMENTATION AND CLASSIFICATION EXPERIMENTS’:, in Proceedings of the Fourth International Conference on Computer Vision Theory and Applications, Lisboa, Portugal, 2009, pp. 135–141. doi: 10.5220/0001768401350141.

[26] G. Zhao and M. Pietikainen, ‘Dynamic Texture Recognition Using Local Binary Patterns with an Application to Facial Expressions’, IEEE Trans. Pattern Anal. Mach. Intell., vol. 29, no. 6, pp. 915–928, Jun. 2007, doi: 10.1109/TPAMI.2007.1110.